Hydroxyl radical and ozone initiated photochemical reactions of 1,3-butadiene

Xiaoyu Liu, Harvey E. Jeffries*, Kenneth G. Sexton

Department of Environmental Science and Engineering, CB7400, Rosenau Hall, The University of North Carolina at Chapel Hill, Chapel Hill, NC 27599-7400, USA

Abstract

1,3-Butadiene, classified as hazardous in the 1990 Clean Air Act Amendments, is an important ambient air pollutant. Understanding its atmospheric transformation is useful for its own sake, and is also helpful for eliciting isoprene's fate in the atmosphere (isoprene dominates the biogenic emissions in US). In this paper, samples from both hydroxyl- and ozone-initiated photooxidation of 1,3-butadiene were analyzed by derivatization with O- (2,3,4,5,6-pentafluorobenzyl)-hydroxylamine followed by separation and detection by gas chromatography/ion trap mass spectrometry to detect and identify carbonyl compounds. The following carbonyls were observed: formaldehyde, acrolein, glycolaldehyde, glycidaldehyde, 3-hydroxy-propanaldehyde, hydroxy acetone, and malonaldehyde, which can be classified into three categories: epoxy carbonyls, hydroxyl carbonyls, and di-carbonyls. Three non-carbonyls, furan, 1,3-buatdiene monoxide, and 1,3-butadiene diepoxide, were also found. To confirm their identities, both commercially available and synthesized standards were used. To investigate the mechanism of 1,3-butadiene, separate batch reactor experiments for acrolein and 1,3-butadiene monoxide were carried out. Time series samples for several products were also taken. When necessary, computational chemistry methods were also employed. Based on these results, various schemes for the reaction mechanism are proposed. © 1999 Published by Elsevier Science Ltd. All rights reserved.

Keywords: Diene; Photochemical reaction mechanism; Atmospheric chemistry; Computational chemistry; PFBHA

1. Introduction

There has been a substantial growth in our understanding of atmospheric chemistry in the last decade (Atkinson, 1990; Jeffries, 1995; Wayne et al., 1991). It has been shown that in addition to their contributions to ozone formation, the degradation of volatile organic compounds (VOCs) also contributes significantly to the generation of secondary air pollutants, including aldehydes, peroxyacetyl nitrate (PAN), and aerosols. There are still major gaps in our knowledge of the oxidation of some common VOCs. Information on kinetics, photo-

lysis pathways, and the reactivity of di-functional products is especially lacking.

1,3-Butadiene, widely used in the chemical industry as a major component of man-made rubber, is classified as a hazardous air pollutant under the 1990 Clean Air Act Amendments (US EPA). Its potential carcinogenicity (Osterman-Golkar and Bond, 1996; Acquavella, 1996; Kligerman et al., 1996; Thornton-Manning et al., 1997) and mutagenicity (Sorsa et al., 1996; Recio et al., 1996) in humans have been the main concern of many investigations. Sources of 1,3-butadiene in the atmosphere include tobacco smoke, automobile exhaust, and gasoline (Thornton-Manning et al., 1997; Sorsa et al., 1996). Concentrations of butadiene measured in urban air range from 1 to 10 ppb (Cote and Bayard, 1990). A relatively complete understanding of the atmospheric transformations of

---

*Corresponding author.

E-mail address: harvey@unc.edu (H.E. Jeffries)

1,3-butadiene is necessary to integrate its transformations into air quality models for toxic species and to improve regulatory quantitative risk decision-making analysis.

Progress has been made in recent years in understanding the fate of 1,3-butadiene in the atmosphere (Maldotti et al., 1980; Ohta, 1983,1984; Barnes et al., 1990; Skov et al., 1992; Atkinson and Aschmann, 1993; Grosjean et al., 1994a; Atkinson et al., 1994a; Atkinson, 1997). Atkinson (1997) reported that the rate constant of the reaction of 1,3-butadiene with hydroxyl radicals (OH) at 298 K and 760 Torr is 6.66×10^{-11} cm^3 molecule^{-1} s^{-1} and of the reaction with O$_3$ is 6.3×10^{-18} cm^3 molecule^{-1} s^{-1}. The major products identified in the 1,3-butadiene + OH radical reaction are acrolein ($\sim 55\%$) (Maldotti et al., 1980), formaldehyde, and furan (5.3–6.7%) (Ohta, 1984). In the ozone reaction, formaldehyde, acrolein, and glyoxal were identified with yields of 7.2 ± 0.8, 1.7 ± 2.2, and $0.4 \pm 0.3\%$, and four other unidentified carbonyls were detected (Grosjean et al., 1994a). Thus, in the OH-initiated reaction, only 60% of the total carbon has been found, whereas, in the O$_3$-initiated reaction, only 10% of the total carbon was detected. Hence, more work is needed to determine the key atmospheric mechanisms that affect degradation of 1,3-butadiene and the formation of its photochemical products.

In this paper, we report a study of the OH radical-initiated and ozone-initiated reactions of 1,3-butadiene in which we applied an analytical derivative method (O-(2,3,4,5,6-pentafluorobenzyl)-hydroxylamine (PFBHA) coupled with gas chromatography (GC)/ion trap mass spectrometry (MS) separation and detection) that has been successful in identifying multifuntional carbonyls in other studies (Yu et al., 1995,1997; Yu and Jeffries, 1997). In a daytime outdoor chamber experiment that started with oxides of nitrogen and 1,3-butadiene, we have detected and identified several carbonyls, by comparison with their corresponding standards, as well as epoxides and furan. We also performed a nighttime experiment in which ozone was injected at a constant rate into the chamber filled with an initial amount of 1,3-butadiene. Additional batch reactor experiments were conducted in an artificially illuminated Teflon Bag Reactor (TBR) system using hydrogen peroxide as a radical source and oxides of nitrogen with acrolein and 1,3-butadiene monoxide as initial organic reactants. Our work shows that the products in the OH- and O$_3$-initiated 1,3-butadiene experiments include acrolein, 1,3-butadiene monoxide, 1,3-butadiene diepoxide, furan, glycolaldehyde, glyoxal, malonaldehyde (CHOCH$_2$CHO), butendial (CHOCH=CHCHO), C$_4$ unsaturated hydroxy carbonyl, glycidaldehyde, 3-hydroxy-propanaldehyde, and a C$_4$ trione and/or C$_4$ epoxy. Time series of some products have also been determined in the experiments. Possible mechanisms for producing these products are proposed. We also performed some theoretical calculations to justify some of the hypothesized pathways.

2. Experimental section

2.1. Outdoor smog chamber experiments

Outdoor smog chamber experiments were carried out in the University of North Carolina (UNC) 300,000-liter dual outdoor chambers located in Chatham County, North Carolina. Two chambers, side by side, allow us to compare two experiments under different conditions at the same time. Detailed descriptions of the chambers and instruments employed are available (Jeffries et al., 1976).

In the daytime experiment conducted on 19 September 1997, 1.5 ppm V of 1,3-butadiene, and 0.68 ppm of NO were injected into the chamber and 0.06 ppm of isotopic ^{13}C$_3$-acetone was used as gas-phase internal standard. The experiment started at 0650 EDT and ended at 1620 EDT. In the nighttime experiment of 7 October 1997, the amount of 1,3-butadiene injected was 1.1 ppmV. Ozone was injected into the chamber for the duration of the experiment at a constant rate of 0.33 ppmh^{-1}. The experiment started at 1923 EDT, just after sunset, and ended at 0123 EDT, in the early morning of the next day.

Carbonyl samples for PFBHA derivatization analysis were collected by following the method described in Yu et al. (1995). Batch samples were collected from the beginning to the end of the experiments, while time series samples were taken at 30-min. intervals throughout each experiment.

In each experiment, background concentrations of NO$_x$, O$_3$, and hydrocarbons were measured. Carbonyl samples collected by impingers for background measurements were taken one hour before each experiment began.

2.2. Indoor chamber experiments

Indoor experiments were performed in a 250-liter TBR and included OH-initiated 1,3-butadiene, acrolein, 1,3-butadiene monoxide, and 1,3-butadiene diepoxide photodegradations, and O$_3$-initiated 1,3-butadiene, acrolein, and 1,3-butadiene monoxide experiments. The temperature was constant at 25°C and the irradiation was generated by lamps mounted on both sides of the bag in a box enclosure lined inside with aluminum foil. The light sources consisted of a mixture of UVA340, F40BL black, and "Vitalite (full spectrum)" lamps. In each OH-initiated experiment, the amount of hydrocarbon injected was about 10 ppmV and that of NO about 10 ppm. To provide a strong OH radical source, the headspace over a 30% H$_2$O$_2$ solution was blown into the bag by zero air at flow rate of 1 l min^{-1} for 15 min. After the initial conditions were established, lights were turned on and remained on until the experiment was finished. In

the O_3 initiated experiments, O_3 was generated by pumping zero air into the bag through an O_3 generator. The hydrocarbon injected in each experiment was about 10 ppm V, and O_3 concentration, measured by an O_3 analyzer at the beginning of the experiment was about 0.9 ppm, and at the end was about 0.1 ppm. Batch sampling, which lasted three hours, was synchronously carried out by pumping air from the bag at flow rate of $0.5\,l\,min^{-1}$ through two impingers, each of which contained 10 ml of a $0.25\,mg\,ml^{-1}$ PFBHA-H_2O solution.

Before each experiment, the bag was flushed five times with zero air from a gas cylinder and background conditions were then checked. Each experiment was repeated at least two times.

2.3. Carbonyl standards preparation and PFBHA derivatives analysis

Many of the carbonyl standard compounds were purchased from Aldrich. The glycidaldehyde standard was produced by photooxidation of 1,3-butadiene monoxide with OH radical without isolation. 3-hydroxy-propanaldehyde was synthesized by photooxidation of 3-buten-1-ol with the OH radical and O_3, without purification. Malonaldehyde was synthesized immediately before usage by hydrolysis of 1,1,3,3-tetraethoxypropane (TEP) in $2\,mol\,l^{-1}$ hydrochloric acid for 90 min without purification (Gutteridge, 1975; Bond et al., 1980). A total of 62 standards have been employed and tested by PFBHA derivatization followed by analysis with Saturn II GC ion trap MS under both chemical ionization (CI) and electron ionization (EI) modes.

The details of the PFBHA derivative method and GC/ion trap MS analysis conditions have been reported elsewhere (Yu et al., 1995,1997). The extraction solvent used in this study was CH_2Cl_2/C_6H_{14} (1 : 4, v : v), and the column used was a $60\,m \times 0.32\,mm \times 0.50\,\mu m$ DB-5 MS-grade, chemically bonded, fused-silica capillary column (J and W Scientific).

2.4. Theoretical procedures

In many cases, neither commercial standards nor synthesized compounds were available. To explore the reaction mechanisms in these cases, we resort to theoretical means, namely, computational chemistry methods. A semiempirical method of modern quantum chemistry, AM1 (Austin Model 1), was used first (Dewar et al., 1985). Due to its use of empirical parameters, this method is suitable only as a screening tool. Where warranted, higher level computational chemistry approaches, such as ab initio (e.g., Hartree-Fock (H-F)) and density functional theory (DFT) methods, have been employed (Frisch et al., 1995). These approaches enable us to calculate the enthalpy difference (ΔH) of a reaction, indicating the thermodynamic tendency of the reaction. If ΔH is nega-

tive, it is more likely that the proposed pathway may occur. Two systems have been investigated by theoretical means in this study. One is the decay of 1,3-butadiene monoxide. The second system is the formation of malonaldehyde. In each of these cases, a mechanism was proposed and then justified by theoretical results. In these calculations, entropy contributions have been neglected. Another factor also neglected in our study is the dynamic properties of the system. These relate to the reaction barrier and thus the reaction rate.

3. Results and discussion

As reported in previous studies (Yu et al., 1995,1997), characteristic fragment ions of the PFBHA-carbonyl derivative include M-181 ($-C_6F_5CH_2$), M-197, ($-C_6F_5CH_2O$), M-211 ($-C_6F_5CH_2ON$), M-167 ($-C_6F_5$), and M-30 ($-NO$). An adductive ion of M + 181 ($+ C_6F_5CH_2$, resulting from secondary ion-molecular reactions of abundant $C_6F_5CH_2$ with targets in the ion trap mass spectrometer) can also be observed. In addition, if the target is a multifunction carbonyl, such as a hydroxy carbonyl, the strong ion peak M-17 ($-OH$) can usually be observed. Carbonyl derivatives containing no hydroxyl group can also show a peak at M-17, but the peak is not as strong as that of the hydroxy carbonyls. Under the CI mode, when methane was used as the CI reagent, extra peaks at M + 1, M + 29, and M + 41 resulted from the addition of H, $C_2H_5^+$, and $C_3H_5^+$ can usually be observed.

GC ion trap MS analysis combined with PFBHA derivatization gives a very good measurement of the molecular weight of an unknown carbonyl. It cannot, however, distinguish one isomer from another. To overcome this problem, commercial standards or synthesized compounds are used to refine the results obtained. Criteria employed in determining the identity of a compound is that its GC retention time and its MS spectra should match those of a standard. Fig. 1 shows a typical result of this procedure. The figure shows a mass chromatogram for the m/z 181 ion, which, because it is a common fragment in all PFBHA derivatives, allows the carbonyl-containing compounds to be identified. On the top of the figure is the chromatogram from the TBR experiment of OH-initiated acrolein photooxidation. One of the unknown peaks marked by arrows has a derivative molecular weight of 267 and three unknown peaks have derivative molecular weights of 462. The 267-peak could be a mono-derivative of a dicarbonyl with a molecular weight of 72. The 462-peaks that appear later in the chromatogram could be the di-derivative of this same carbonyl. Possible dicarbonyl candidates are malonaldehyde and methylglyoxal, which have the same mass. Their GC chromatograms are plotted in the middle and at the bottom of the same figure. It is seen that
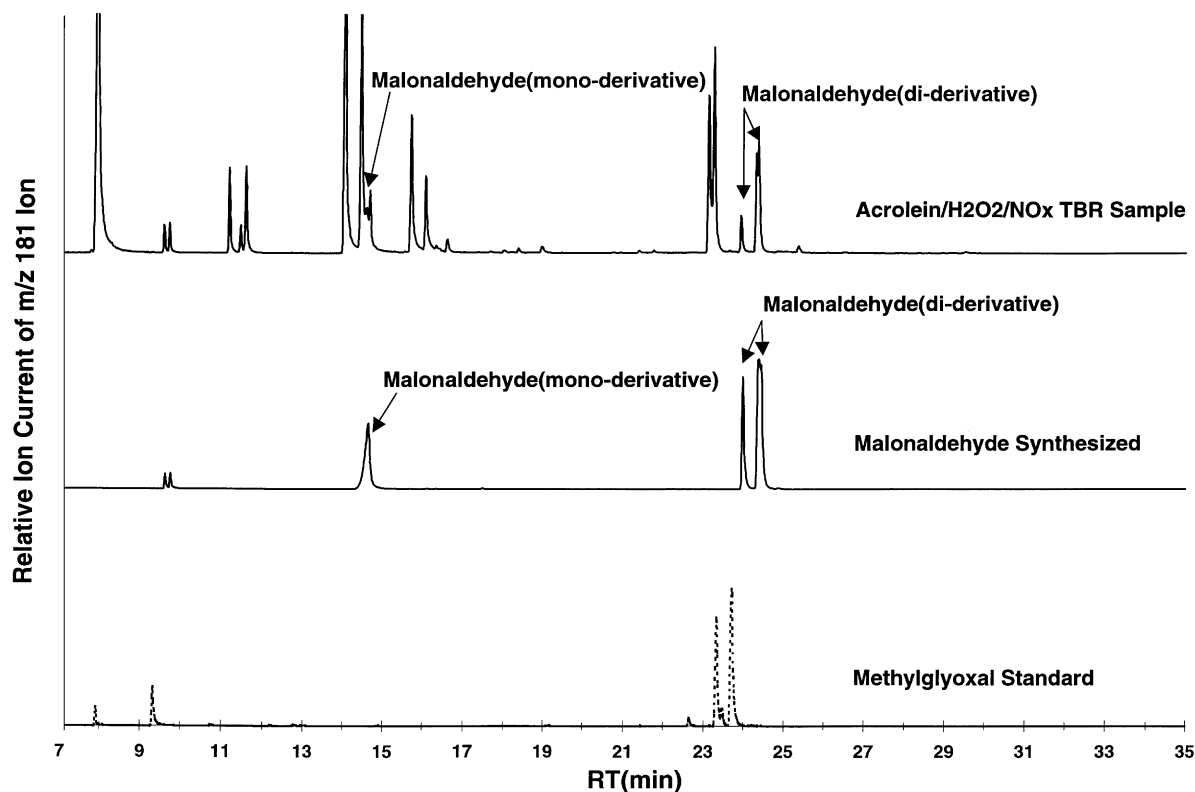
Fig. 1. Acrolein/H$_2$O$_2$/NO$_x$ TBR experiment results compared with methylglyoxal standard and synthesized malonaldehyde. Top: acrolein TBR experiment. Middle: synthesized malonaldehyde standard. Bottom: methylglyoxal standard. Y-axis: relative ion current of m/z181 ion. X-axis: retention time in min.

malonaldehyde's retention times match very well with those of the four unknown peaks. The combination of the mass spectra and the GC retention times is taken as confirmation of the identity of the unknown compound in the chamber sample.

Results from both the outdoor and indoor experiments for the same VOC were very similar. Differences originate from the different size of the reactor and the different light sources. The latter is especially important for photoreactive species, such as α-dicarbonyl and unsaturated carbonyls. The outdoor chamber uses sunlight, so the results of the 1,3-butadiene experiments shown here are from the outdoor smog chamber. The chamber conditions, including air temperature, dew point temperature, Eppley total solar radiation (TSR)/Eppley ultraviolet radiation (UV), and concentrations of NO$_x$ and O$_3$ on 19 September 1997 and 7 October 1997 are shown in Figs. 2 and 3. For the experiment conducted on 7 October 1997 (Fig. 3), O$_3$ was injected into both sides of the dual chamber continuously, but only one side contains 1,3-butadiene. By comparing the time profile of O$_3$ injected into the blank side of the chamber with the time profile of O$_3$ injected into the other side of the chamber

containing 1,3-butadiene. One can determined the O$_3$ consumed in the reaction.

3.1. Products analysis in 1,3-butadiene experiments

Carbonyl products detected and identified in the OH-initiated 1,3-butadiene daytime chamber experiment are shown in Fig. 4 and are listed in Table 1. Since the purity of reactant is 99% and the background was measured before the experiment, we conclude that these major carbonyl products are most likely from 1,3-butadiene or its products. Formaldehyde, acrolein, glycolaldehyde, glycidaldehyde, glyoxal, butendial, 3-hydroxy-propanaldehyde, hydroxy acetone, and malonaldehyde were found and confirmed by matching their retention times and mass spectra with standards. Among these identified compounds, acrolein and formaldehyde have previously been reported by Maldotti et al. (1980) and Ohta (1984). The new carbonyls we found can be classified into three categories according to their different functional groups: epoxy carbonyl (glycidaldehyde), hydroxyl carbonyls (glycolaldehyde, 3-hydroxy-propanaldehyde, and hydroxy acetone), and di-carbonyls (glyoxal, butendial,
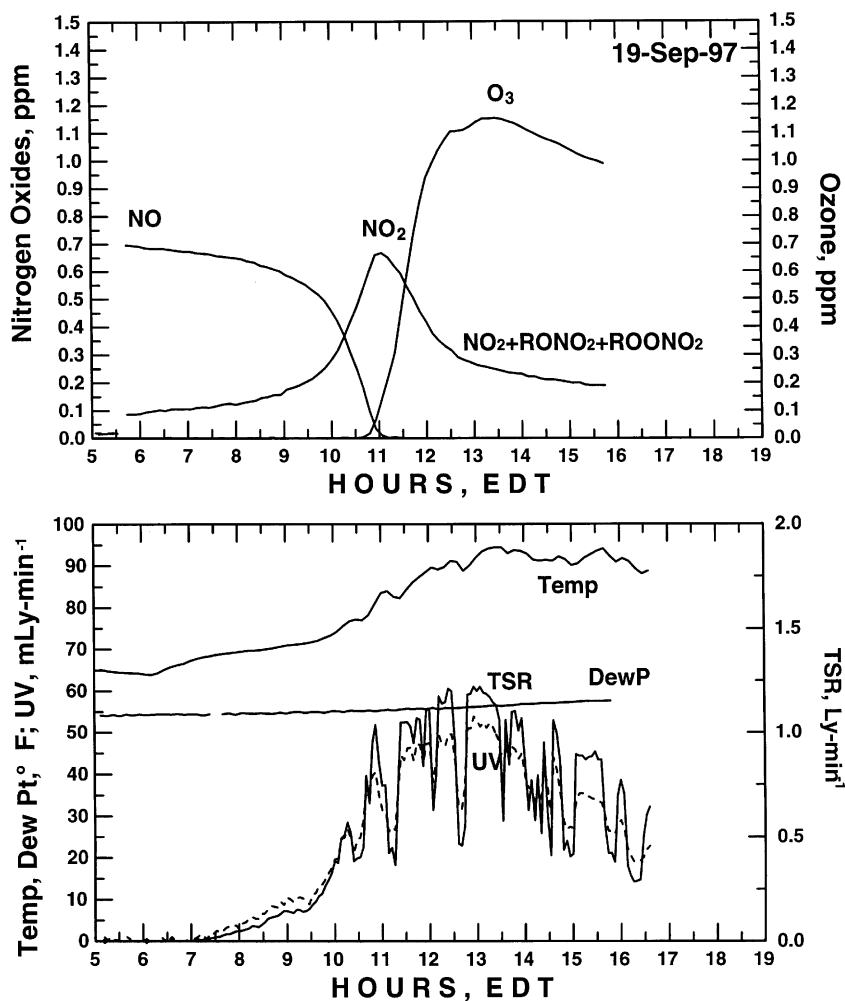
Fig. 2. Daytime outdoor dual smog chamber experiment using 1.5 ppmV 1,3-butadiene and 0.68 ppm nitrogen oxides. Top: NO, NO_2, O_3 time profiles. Bottom: Temp-chamber air temperature, DewP-chamber dew point temperature, TSR-Eppley total solar radiation, UV-Eppley ultraviolet radiation.

and malonaldehyde). In addition, three non-carbonyl VOCs were also identified: furan, 1,3-butadiene monoxide, and 1,3-butadiene diepoxide. Identification of these compounds was made by gas chromatographs using gas-phase samples drawn directly from the chamber and by confirmation using standards injected into the chamber in separate experiments not shown here.

Also shown in Table 1 and Fig. 4 are carbonyl compounds whose identities are not unambiguously determined because of the lack of standards. Peaks BD7 and BD8 share the same derivative molecular weight of 265, representing C_4 unsaturated carbonyls. Three standards, methyl vinyl ketone, methylacrolein, and crotonaldehyde, have been tested and none matched retention times of the unknowns. Peaks BD15, BD16, and BD20 have strong fragment peaks at M-17, and their derivative

molecular weights are 281. These may be isomers of C_4 unsaturated hydroxy carbonyls or C_4 epoxy carbonyls. Peaks BD17 and BD18 have a derivative molecular weight of 267, possibly a C_3 dicarbonyl, C_3 epoxy carbonyl, C_4 saturated carbonyl, or C_3 unsaturated hydroxy carbonyl. We did not observe M-17 ion peaks in their mass spectra, and their retention times do not match those of isobutyraldehyde, butyraldehyde, methyl ethyl ketone, glycidaldehyde, methylglyoxal (mono-derivative), and malonaldehyde (mono-derivative). Peaks BD27 and BD28, which have a derivative molecular weight of 490, may be either C_4 triones or C_4 epoxy dicarbonyls. For Peaks BD29 and BD30, with a derivative molecular weight of 478, C_3 hydroxy dicarbonyls are the only option.

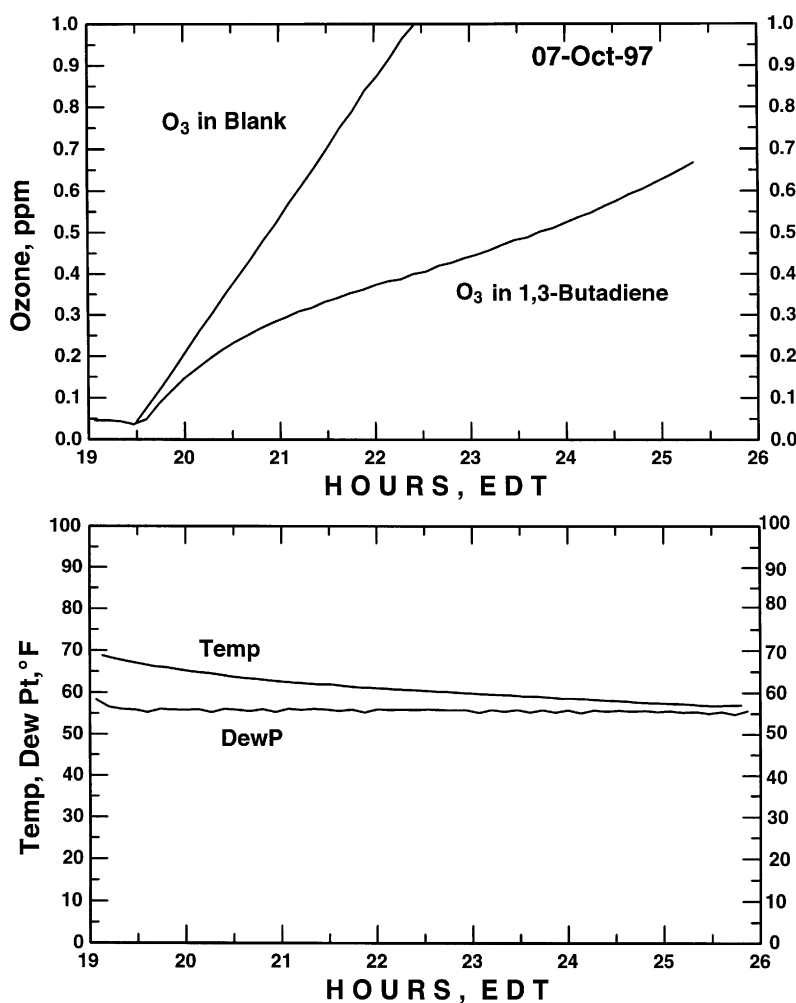Carbonyl products identified in the O_3-initiated 1,3-butadiene nighttime chamber experiment are shown in

Fig. 3. Nighttime outdoor dual smog chamber experiment using 1.5 ppmV 1,3-butadiene and O_3 at 0.33 ppm hr^{-1}. Top: O_3 in blank: time profile of O_3 injected into the blank side of the chamber, O_3 in 1,3-butadiene: time profile of O_3 injected into the other side of the chamber containing 1,3-butadiene. Bottom: Temp-chamber air temperature, DewP-chamber dew point temperature.

Fig. 5 and Table 2. Most of the carbonyl products detected are the same as in the daytime OH-initiated experiment. Exceptions are 2,3-butadione (Peaks BN19, BN20, and BN25) and Peak BN27, which is a co-elute of compounds with derivative molecular weights of 476 and 490. The 476 peak is possibly a C_4 saturated dicarbonyl or a C_3 trione, while the 490-peak may be either a C_4 trione or a C_4 epoxy dicarbonyl. In another study (Grosjean, 1994a), three known carbonyls, namely, formaldehyde, acrolein, and glyoxal, have been reported, plus four unknown carbonyls. The three known carbonyls are included in Table 2, and the four unknown carbonyls may be any of the others listed in the table.

Three non-carbonyl VOCs, furan, 1,3-butadiene monoxide, and 1,3-butadiene diepoxide, found in the daytime experiment have also been found in the nighttime cham-

ber experiment. This observation confirms the finding of Atkinson and Aschmann (1993) that reaction of O_3 leads to formation of 1,3-butadiene monoxide. Moreover, our results show that furan identified in the OH-initiated photooxidation (Ohta, 1984) is also found in the O_3-initiated reaction. In both cases, we report for the first time the existence of 1,3-butadiene diepoxide.

3.2. Products analysis in acrolein and 1,3-butadiene monoxide experiments

Acrolein and 1,3-butadiene monoxide are both products of the oxidation of 1,3-butadiene. Both products can react further during 1,3-butadiene photodegradation with the hydroxyl radical and with O_3. Separate investigations of the fates of these two compounds are needed

Table 1
Carbonyl products detected in the batch sample collected from 1,3-butadiene daytime outdoor smog chamber experiment

Peak	RT (min)	Identity	MW[a]	FW[b]
BD1	7.99	Formaldehyde	225	30
BD2/BD3	9.73/9.86	Acetaldehyde	239	44
BD4/BD5	11.31	Acrolein	251	56
BD6	11.73	Glyoxal (mono-derivative)	253	58
BD7/BD8	12.71/12.77	C4 unsaturated carbonyl	265	70
BD9	14.18	Glycolaldehyde	255	60
BD10	14.58	Glycolaldehyde/Glycidaldehyde	255/267	60/72
BD11	14.71	Malonaldehyde (mono-derivative)	267	72
BD12	14.81	Glycidaldehyde	267	72
BD13	14.96	Hydroxy acetone	269	74
BD14	15.86	3-hydroxy-propanaldehyde	269	74
BD15/BD16	16.21/16.41	C4 unsaturated hydroxy carbonyl, C4 epoxy carbonyl	281	86
BD17/BD18	17.66/17.79	C4 saturated carbonyl, C3 unsaturated hydroxy carbonyl	267	72
BD19	18.26	PHBCHO	391	196
BD20	18.83	C4 unsaturated hydroxy carbonyl, C4 epoxy carbonyl	281	86
BD21/BD22	23.24/23.38	Glyoxal	448	58
BD23	23.78	Methylglyoxal	462	72
BD24/BD25/BD26	24.08/24.46/24.51	Malonaldehyde	462	72
BD27	25.47/25.53	C4 trione, C4 epoxy dicarbonyl	490	100
BD28	25.68/25.75	C4 trione, C4 epoxy dicarbonyl	490	100
BD29/BD30	26.04/26.23	C3 hydroxy dicarbonyl	478	88
BD31/BD32/BD33	26.59/26.91/27.04	Butendial	474	84
BD34/BD35	27.23/32.29	Butendial	474	84

[a]Molecular weight of PFBHA derivative.
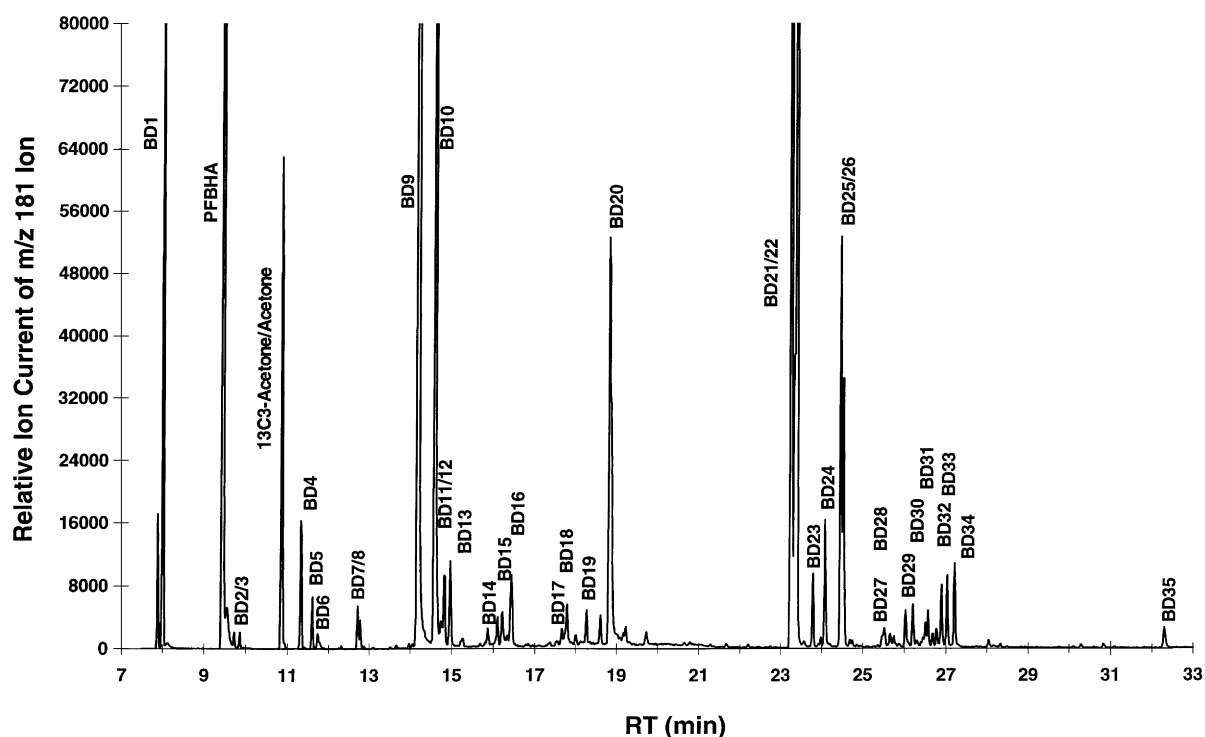[b]Molecular weight of carbonyl compound.

Fig. 4. Reconstructed m/z 181 ion chromatogram of a batch sample collected from 1,3-butadiene daytime outdoor smog chamber experiment. Y-axis: relative ion current of m/z181 ion. X-axis: retention time in min.
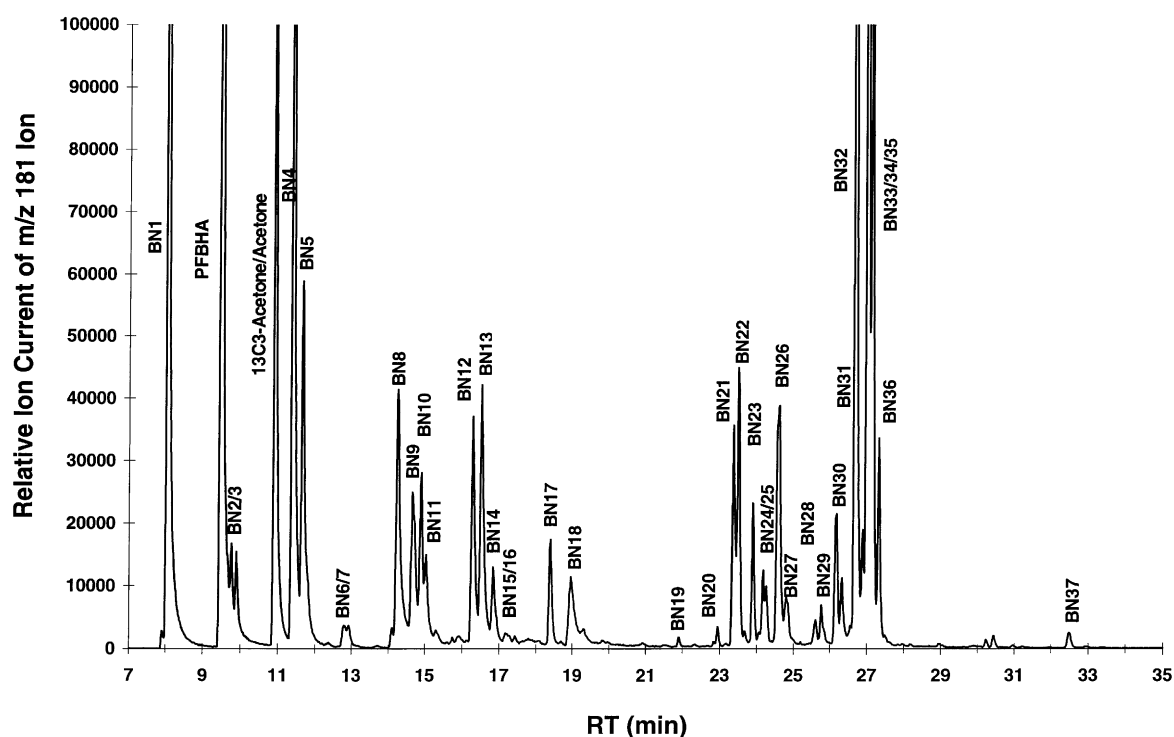
Fig. 5. Reconstructed *m/z* 181 ion chromatogram of a batch sample collected from 1,3-butadiene nighttime outdoor smog chamber experiment. Y-axis: relative ion current of *m/z*181 ion. X-axis: retention time in min.

Table 2
Carbonyl products detected in the batch sample collected from 1,3-butadiene nighttime outdoor smog chamber experiment

Peak	RT (min)	Identity	MW[a]	FW[b]
BN1	8.03	Formaldehyde	225	30
BN2/BN3	9.76/9.89	Acetaldehyde	239	44
BN4/BN5	11.38/11.64	Acrolein	251	56
BN6/BN7	12.81/12.89	C4 unsaturated carbonyl	265	70
BN8	14.24	Glycolaldehyde	255	60
BN9	14.64	Glycolaldehyde/Glycidaldehyde	255/267	60/72
BN10	14.89	Glycidaldehyde	267	72
BN11	15.03	Hydroxy acetone	269	74
BN12/BN13/BN14	16.28/16.51/16.84	C4 unsaturated hydroxy carbonyl, C4 epoxy carbonyl	281	86
BN15/BN16	17.16/17.43	Butendial (mono-derivative)	279	84
BN17	18.39	PFBCHO	391	196
BN18	18.95	C4 unsaturated hydroxy carbonyl, C4 epoxy carbonyl	281	86
BN19/BN20	21.91/22.94	2,3-Butadione	476	86
BN21/BN22	23.36/23.49	Glyoxal	448	58
BN23	23.89	Methylglyoxal	462	72
BN24	24.18	Malonaldehyde	462	72
BN25	24.26	2,3-Butadione	476	86
BN26	24.53/24.59	Malonaldehyde	462	72
BN27	24.79	C4 dicarbonyl,C3 trione, C4 trione, C4 epoxy dicarbonyl	476/490	86/100
BN28/BN29	25.61/25.76	C4 trione, C4 epoxy dicarbonyl	490	100
BN30/BN31	26.18/26.33	C3 hydroxy carbonyl	478	88
BN32/BN33/BN34	26.7/26.89/27.01	Butendial	474	84
BN35/BN36/BN37	27.14/27.33/32.49	Butendial	474	84

[a]Molecular weight of PFBHA derivative.
[b]Molecular weight of carbonyl compound.

to complete the fate of their parent compound. To this end, TBR experiments of acrolein/H_2O_2/NO_x and 1,3-butadiene monoxide/H_2O_2/NO_x have been carried out. The products observed and identified are shown in Fig. 6 and Table 3. Carbonyl products found in the acrolein/H_2O_2/NO_x experiment are formaldehyde, glyoxal, glycolaldehyde, glycidaldehyde, malonaldehyde, 3-hydroxy-propanaldehyde, and possibly a C_3 trione. The products in the 1,3-butadiene monoxide TBR experiment are almost the same as those of 1,3-butadiene.

The atmospheric chemistry of acrolein has been investigated in a few recent studies (Grosjean et al., 1994b; Grosjean, 1990). Two carbonyl compounds, formaldehyde and glyoxal, were reported by Grosjean (1990). In another study, Grosjean et al. (1994b) identified a third carbonyl, glycolaldehyde (hydroxyacetaldehyde), both in the reaction of acrolein with ozone in the dark and in sunlight irradiation of the acrolein–NO mixture. In contrast, photochemical behavior of 1,3-butadiene monoxide is essentially unknown. The only literature found was a report by Atkinson and Aschmann (1993), showing that 1,3-butadiene monoxide is a direct product of 1,3-butadiene O_3 photooxidation, with a yield of about 5%.

3.3. Quantification

While the UNC outdoor smog chamber provides for photochemical reactions to occur under realistic physical conditions and can provide large samples used to identify products and intermediates during the course of reactions, it is difficult to measure reaction yields under these conditions. The products formed during the reaction continue to undergo further photochemical processes, either via photolysis or by reacting with the OH radical, NO_x, O_3 or other radicals and we cannot "turn out the lights" to stop the reaction when product concentrations are measured. One can, however, measure the time series of a product during the reaction process and thus gain insight into pathways and relative rates. The time series of a carbonyl is represented by its relative concentration defined as the area ratio of the m/z 181-ion peak of the carbonyl to the m/z 59-ion peak of $^{13}C_3$-acetone. This technique is quite useful when a series of related compounds are plotted together in the same figure. From the curves, one sees how reactants are consumed, intermediates are first produced and then decayed, and what final or stable products are eventually formed. This
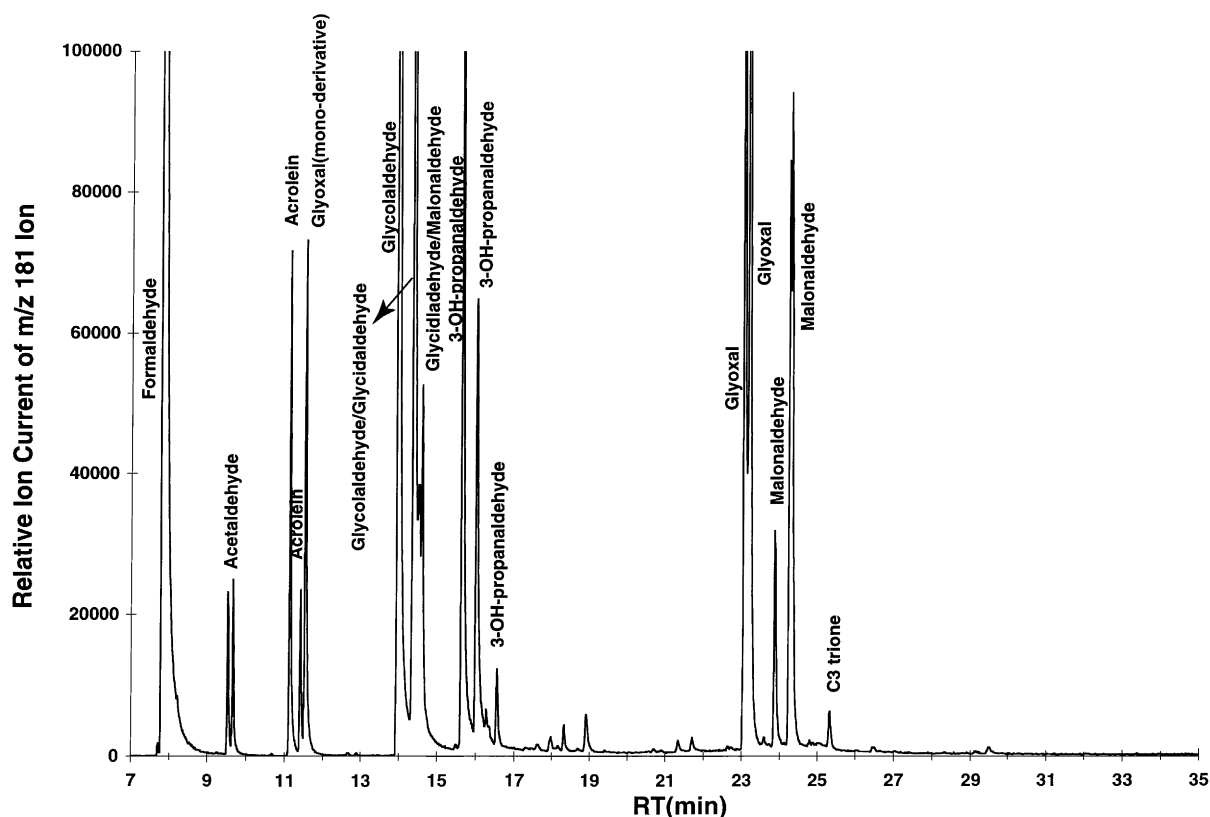

Fig. 6. Reconstructed m/z 181 ion chromatogram of a batch sample collected from acrolein indoor TBR experiment. Y-axis: relative ion current of m/z181 ion. X-axis: retention time in min.

Table 3
Carbonyls Products Detected in the Batch Sample Collected from 1,3-Butadiene Monoxide/H_2O_2/NO_x TBR Experiment

Peak	RT (min)	Identity	MW[a]	FW[b]
BM1	7.81	Formaldehyde	225	30
BM2/BM3	9.53/9.66	Acetaldehyde	239	44
BM4/BM5	11.11/11.39	Acrolein	251	56
BM6	11.53	Glyoxal (mono-derivative)	253	58
BM7/BM8	12.5/12.56	C4 unsaturated carbonyl	265	70
BM9	13.94	Glycolaldehyde	255	60
BM10	14.38	Glycolaldehyde/Glycidaldehyde	255/267	60/72
BM11	14.53	Glycidaldehyde/Malonaldehyde(mono-derivative)	267	72
BM12	14.61	Glycidaldehyde	267	72
BM13	15.63	3-hydroxy-propanaldehyde	269	74
BM14	15.99	3-hydroxy-propanaldehyde/C4 unsaturated hydroxy carbonyl, C4 epoxy carbonyl	269/281	74/86
BM15	16.26/16.31	C4 unsaturated hydroxy carbonyl, C4 epoxy carbonyl	281	86
BM16	17.11	Butendial (mono-derivative)	279	84
BM17	18.08	PFBCHO	391	196
BM18/BM19	18.59/18.66	C4 unsaturated hydroxy carbonyl, C4 epoxy carbonyl	281	86
BM20/BM21	23.06/23.19	Glyoxal	448	58
BM22/BM23	23.86/24.24/24.31	Malonaldehyde	462	72
BM24/BM25	24.88/25.29	C4 dicarbonyl, C3 trione	476	86
BM26/BM27	25.48/26.01	C3 hydroxy dicarbonyl	478	88
BM28	26.18	C4 hydroxy dicarbonyl	492	102
BM29/BM30/BM31	26.38/26.58/26.69	Butendial	474	84
BM32/BM33/BM34	26.83/27.01/32.03	Butendial	474	84

[a] Molecular weight of PFBHA derivative.
[b] Molecular weight of carbonyl compound.

information is helpful in understanding and proposing reaction mechanisms. Eventually, the reaction yields can be estimated by simulation studies. As we will show later, the observed curves can also help us to identify different kinds of unknown isomers.

Plotted in Figs. 7–10 are time series of 1,3-butadiene and some of its products in both the daytime and nighttime experiments. In the daytime experiment (Fig. 7), as 1, 3-butadiene was reacted, acrolein and 1,3-butadiene monoxide concentrations quickly increased in the morning before a large amount of O_3 was formed (see Fig. 2). They then began to be steadily consumed by the increasing O_3 and the OH radical. Glycolaldehyde (Fig. 8) was found to be relatively stable after its formation; glycidaldehyde, however, seems to decline beginning at about the same time as the butendial.

In Fig. 9, time series of three GC peaks, BD15, BD16, and BD20, in the 1,3-butadiene daytime outdoor smog chamber experiment are shown. These three peaks share the same derivative molecular weight of 281, representing C_4 unsaturated hydroxy carbonyls or C_4 epoxy carbonyls. From the time series data, two distinct patterns can be observed. One is BD15 and BD16. The similar time series curves of BD15 and BD16 may indicate that they are the PFBHA derivative isomers of the same

carbonyl. The other is the BD20 peak, suggesting that BD20 is a different carbonyl. It is thus believed that the 281-peaks correspond to at least two distinct carbonyl products.

Nighttime (O_3) series are shown in Fig. 10 for 1,3-butadiene, acrolein, and 1,3-butadiene monoxide. It is found that as the reactant is steadily consumed, the two products exhibit a monotonic buildup. This characteristic is rather different from what has been observed in the daytime series (Fig. 7). This is because in the nighttime experiment, O_3 was continuously added into the reactor and there was no photolysis pathway available for acrolein, while in the daytime experiment, NO was added at the beginning of the experiment and three pathways were available for acrolein to react, that is, via reaction with O_3, via reaction with OH, and via its own photolysis.

Quantitative measurements were also made for non-carbonyls. Furan and 1,3-butadiene diepoxide in the daytime experiments are the two non-carbonyls detected by the Varian 3400 GC-FID. Unfortunately, the 2-h sampling frequency did not provide sufficient time resolution for time series plots. The highest observed concentration of furan was about 0.02 ppm C, and that of 1,3-butadiene diepoxide about 0.01 ppm C. The concentrations of
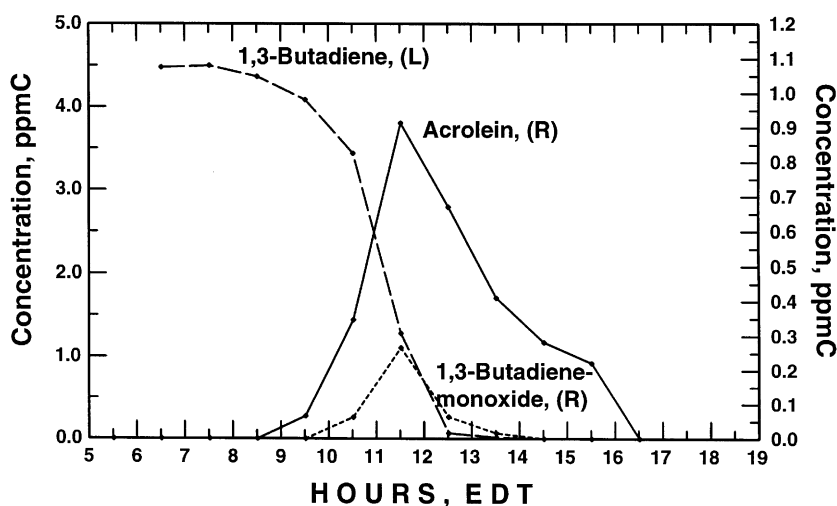
Fig. 7. Time series of acrolein and 1,3-butadiene monoxide in 1,3-butadiene daytime outdoor smog chamber experiment. R: right Y-axis. L: left Y-axis.
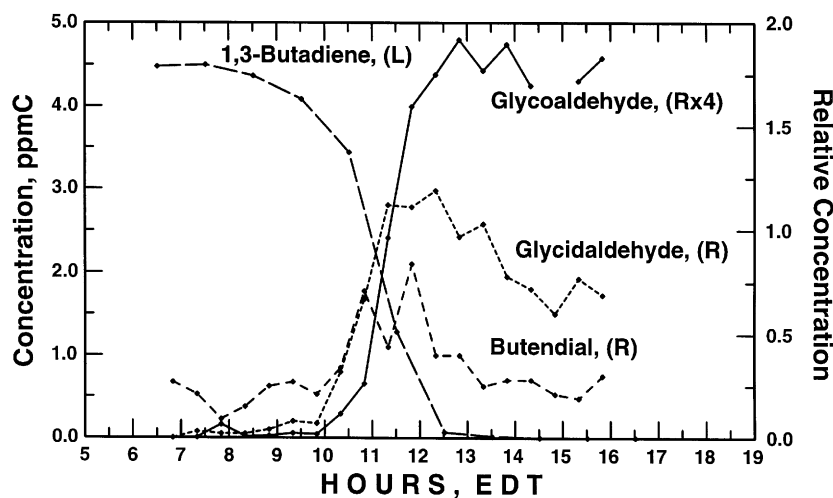

Fig. 8. Time series of glycidaldehyde, glycolaldehyde, butendial in 1,3-butadiene daytime outdoor smog chamber experiment. R: right Y-axis. L: left Y-axis. Rx4: scale is 4 times of the right Y-axis.

1,3-butadiene diepoxide and furan in the nighttime experiment are less than those in the daytime run, and close to the detection limit. Hence, no quantification data are available.

3.4. OH initiated 1,3-butadiene reaction mechanisms

The OH-initiated photooxidation reaction of 1,3-butadiene in the presence of NO_x might be expected to be analogous to the isoprene reaction. The absence of a methyl group and presence of a higher symmetry in 1,3-butadiene, however, leads to a simpler set of reaction products that significantly simplify the estimation of its complete reaction mechanism.

Hydroxyl radical addition to the $>C=C-C=C<$ system is predominately expected to occur at the 1- and/or 4-positions, leading to formation of thermochemically favored alkyl radicals (Atkinson, 1997; Carter, 1996). The subsequent reactions of these radicals have been reported via following channels: O_2 addition, converting NO to
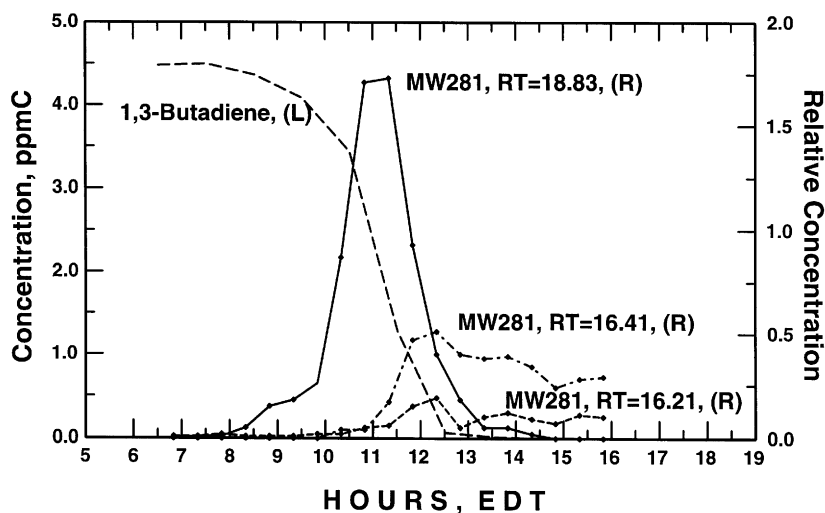
Fig. 9. Time series of MW281 carbonyls in 1,3-butadiene daytime outdoor smog chamber experiment. R: right Y-axis. L: left Y-axis.
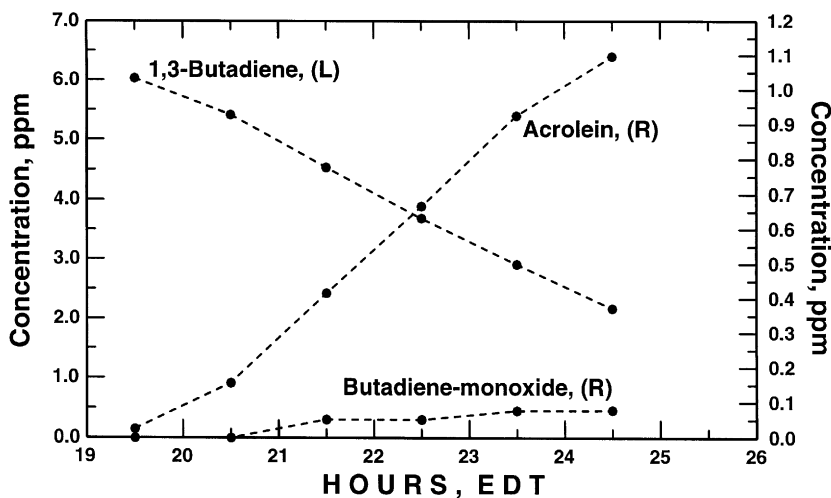

Fig. 10. Time series of acrolein, 1,3-butadiene monoxide in 1,3-butadiene nighttime outdoor smog chamber experiment. R: right Y-axis. L: left Y-axis.

NO_2, leading to the formation of the alkoxy radicals, followed by unimolecular decomposition, H abstraction, and isomerization. Identification of 1,3-butadiene monoxide and 1,3-butadiene diepoxide before O_3 was produced in the OH-initiated reaction suggests that a different pathway than suggested by Atkinson and Aschmann (1993) might be occurring. From Figs. 2 and 7, we can see that even in the morning (9:30–11:00 am), about 0.1 ppm C 1,3-butadiene monoxide was observed. Because NO_2 concentration is high at this time, its formation may be from 1,3-butadiene reacting with

O (^3P) resulted from the photolysis of NO_2 (Paulson et al., 1992a).

To explain the similarity of carbonyl products among 1,3-butadiene monoxide and diepoxide, and 1,3-butadiene, we proposed that the oxane ring in 1,3-butadiene monoxide and diepoxide could be opened by an OH attack, forming a hydroxy alkoxy radical. Computational chemistry calculations show that enthalpy changes of 1,3-butadiene monoxide with OH reactions (Reaction Scheme 1) are about -50 kcal mol^{-1} at the AM1 level and around -40 kcal mol^{-1} at DFT non-local
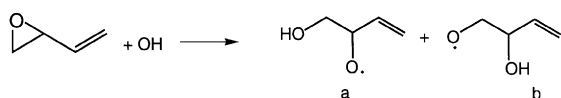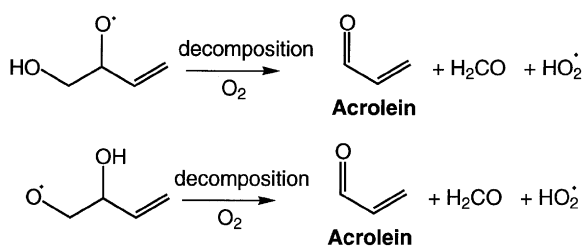
Reaction scheme 1.

Reaction scheme 3.

B3LYP/6-31G(d, p) level, indicating energetic favorablity of these reactions. To have a quantitative picture of these reactions, however, more study is needed to theoretically predict their transition states and reaction barriers so that their dynamic properties may be investigated.

Three peaks with derivative molecular weights that correspond to C_4 unsaturated hydroxy carbonyls or other isomers have also been observed. Since none of their standards are available, we were unable to confirm their structures. Time series of these peaks are shown in Fig. 9, and suggest that these three peaks belong to at least two different compounds. One of the carbonyls was formed earlier in the morning, and had its highest concentration at about 10:30–11:00 am before a large amount of O_3 was generated in the chamber, and then quickly decreased. The other two were formed later than the first, coincident with the O_3 built-up in the day, and remained relatively stable after their formation compared with the first one. One of the possible pathway and structure of the first compound was given in Reaction Scheme 2. Addition of an OH radical to the 1, or 4 position of 1,3-butadiene forms a δ-hydroxyalkyl radical. This radical reacts with O_2 and converts NO to NO_2 to produce a hydroxyalkoxy radical (RO•). H-abstraction of the unsaturated hydroxyalkoxy radical by O_2 leads to a C_4 unsaturated hydroxy carbonyl. This reaction is an important source for converting NO to NO_2, which is the cause of the ozone formation.

Acrolein is formed from OH addition to the 1 or 2 position of 1,3-butadiene, followed by decomposition of β- hydroxyalkoxy radicals (Reaction Scheme 3). It is one of the major carbonyl products with a previously reported yield of about 55% (Maldotti et al., 1980). Its time series during the daytime experiment (Fig. 7) indicates that it was a primary product and, after its formation, it both reacts with other species (e.g., OH, O_3, HO_2) in the chamber and undergoes photolysis. It has been reported (Finlayson-Pitts and Pitts, 1986) that acrolein mainly reacts with OH by H-atom abstraction at the carbonyl carbon site, and reacts with OH and O_3 by addition at the double bond. The products found by Grosjean et al. (1994b) (see also Grosjean, 1990) include formaldehyde, glyoxal, glycolaldehyde, and unsaturated peroxyacyl

nitrate. In our acrolein/NO_x/H_2O_2 experiment, the products identified were formaldehyde, glyoxal, glycolaldehyde, glycidaldehyde, malonaldehyde, 3-hydroxypropanaldehyde. In addition, a peak with molecular weight that corresponds to a C_3 trione was detected.

Glycolaldehyde and glyoxal are secondary products of C_4 unsaturated hydroxy carbonyl oxidation and of acrolein (Reaction Scheme 4). Decomposition of hydroxy alkoxy radicals could also generate glycolaldehyde.

Also observed in the experiment is glycidaldehyde, a C_3 epoxy carbonyl with the aldehyde group adjacent to an epoxy group. Glycidaldehyde has also been reported as a product of aromatic species oxidation (Yu and Jeffries, 1997). Its possible pathways of formation are outlined in Reaction Scheme 5. In this scheme, the last alternative channel is via acrolein reacting with O_3. This reaction could have become more important as O_3 was gradually produced in the OH reaction system. Glycidaldehyde was found to be a potent mutagen in a variety of in vitro test systems and shown to induce sarcomas in rats by subcutaneous injection due to its bifuctional chemical character (Golding et al., 1990,1996; Knaap et al., 1982; McCann et al., 1975).

Another carbonyl detected in the OH-initiated photooxidation reaction of 1,3-butadiene was butendial, which can be formed via OH radical reacting with furan (Reaction Scheme 6).
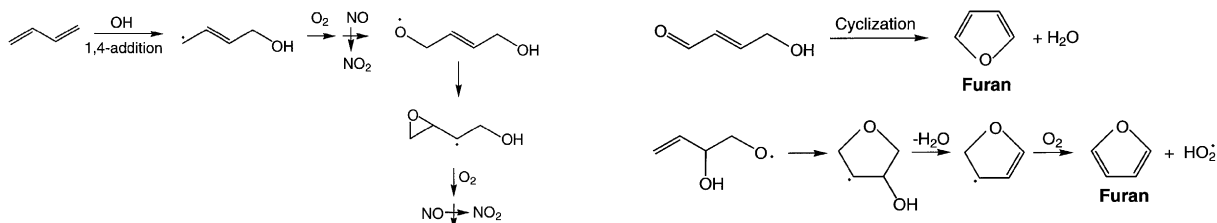
Furan and its substituted variants have been reported in the photooxidation of hydrocarbons with a general structure of CH_2=CH–CR_1=CHR_2 (Bierbach et al., 1995). Butenedial has been found as a major product in furan's atmospheric chemistry, with a total yield up to 70% C of the total carbon balance (Bierbach et al., 1995). It was shown that in the OH initiated 1,3-butadiene experiment, the yield of furan was 5.3–6.7% (Ohta, 1984). Shown in Reaction Scheme 7 are two pathways proposed to explain the formation of furan in the present experiment.
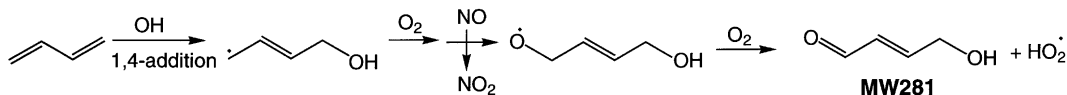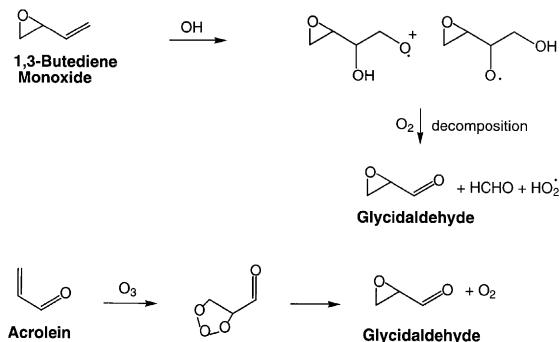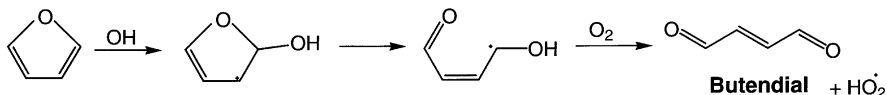

Reaction scheme 2.
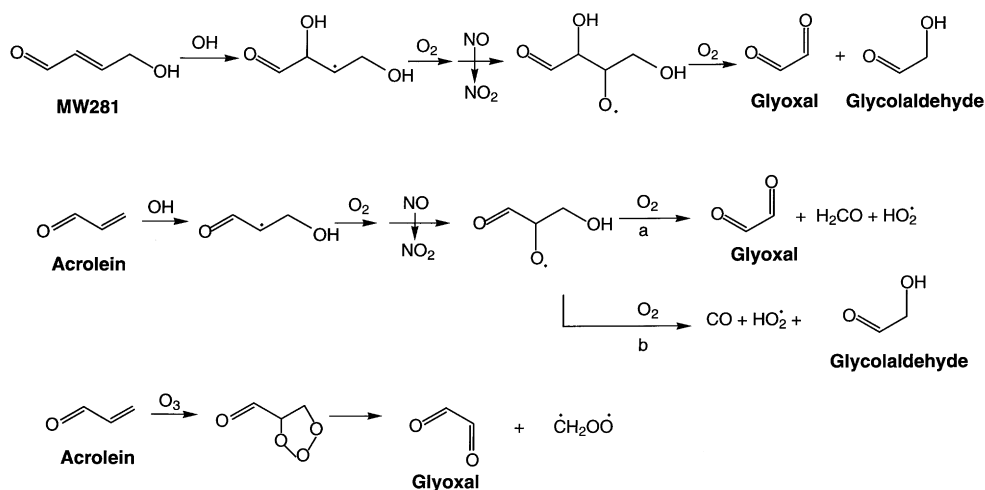
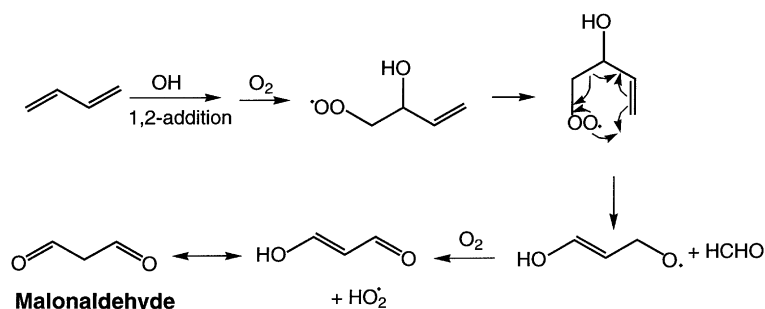Reaction scheme 4.

Reaction scheme 5.

Reaction scheme 7.

over, it is carcinogenic in rats and mutagenic in a number of bacterial and mammalian mutational assays due to its ability to crosslink to proteins and bind covalently to nucleic acids (Fang et al., 1996; Nishiyama et al., 1994; Feron et al., 1991). Besides appearing in the 1,3-butadiene system, other TBR experiments show that this compound has also been identified in the OH-initiated acrolein, 1,3-butadiene monoxide, and 1,3-butadiene diepoxide photooxidation reactions. To produce this compound, a step involving an H-shift must have taken place. To explain the formation of malonaldehyde, Reaction Scheme 8 shows one possible mechanism. The key is Step 4, where the alkyl peroxy radical decomposes into a hydroxy alkoxy radical plus a HCHO. To show that this mechanism is reasonable and this key step is possible, semiempirical AM1, ab initio H-F, and DFT nonlocal calculations have been performed, giving an energy change of -32.2, -32.4, and -18.8 kcal mol^{-1}. These

Formation of malonaldehyde (propandial) found in the current experiment is of special interest. This compound is the major aldehyde resulting from the peroxidation of polyunsaturated fatty acid constituents of biological membranes (Gutteridge, 1975; Bond et al., 1980). More-

Reaction scheme 6.
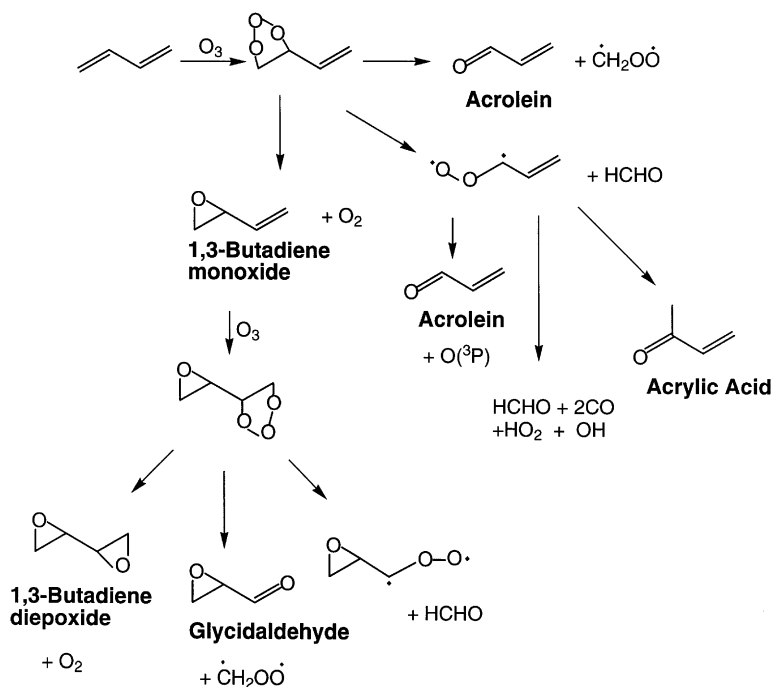
Reaction scheme 8.

theoretical results suggest that the proposed reaction is a possibility.

A peak with a derivative molecular weight of 478 represents a C_3 hydroxyl dicarbonyl. These compounds may form either from C_4 unsaturated hydroxyl carbonyl decomposition or from OH addition to acrolein followed by H abstraction. Possible candidates for the 490 peak are a C_4 trione, C_4 epoxy dicarbonyl, or C_4 unsaturated hydroxy dicarbonyl. Wiesen et al. (1995) and Yu et al. (1997) found vicinal polyketones in the photooxidation of 3-hexene-2, 5-dione and some aromatics. Our result supports the observation that 490 peak is a C_4 trione formed from a C_4 hydroxy dicarbonyl.

3.5. O_3 initiated 1,3-butadiene reaction mechanisms

It is well known that O_3 readily reacts with alkenes and that some of the reactive Criegee biradical fragments decompose to form OH radical (Atkinson et al., 1992; Atkinson, 1997) (and reference therein). The yield of the OH radical generated in the 1,3-butadiene/O_3 system was reported to be 8% (Atkinson et al., 1993). The Criegee biradicals provide a source of the OH radical at night. The fates of the Criegee biradicals and the products they ultimately formed are not clear for higher alkenes.

The 1,3-butadiene and O_3 reaction proceeds by an initial O_3 addition to the $>C=C<$ bond to yield an

Reaction scheme 9.

energy-rich moleozonide, which rapidly decomposes to a carbonyl and a Criegee biradical (Reaction Scheme 9). Since no radical scavenger has been used in our reaction system, the products observed have resulted from reactions of 1,3-butadiene with both O_3 and the OH radical. Since the experiment was conducted in the dark, the products that would have photolyzed during the day will be more stable in these experiments. Our data show that products found in the nighttime experiment are almost the same as in the daytime experiment.

Formation of acrolein, glycidaldehdye, 1,3-butadiene monoxide, and 1,3-butadiene diepoxide can also be explained via 1,3-butadiene reacting with O_3 as shown in Reaction Scheme 9. We observed a peak with a derivative molecular weight of 476, the same as that of 2,3-butadione, but the peak's retention time did not match 2,3-butadione. Alternative structures include a C_3 trione or a C_4 dicarbonyl. This peak may also arise in the same reaction pathway as the C_4 trione. 2,3-Butadione itself was only observed in the nighttime chamber experiment. Different arguments are proposed in the literature (Martinez et al., 1981; Paulson et al., 1992a,1992b; Atkinson et al., 1994a, b) as to how epoxy compounds are formed.

We observed peaks with derivative molecular weights of 279 in our nighttime chamber and O_3 TBR experiments. It corresponds to a C_5 unsaturated carbonyl or the mono derivative of a C_4 unsaturated dicarbonyl. Comparison of its retention time with the butendial standard confirms that it was the mono derivative of butendial. In the literature (Yu et al., 1995), without standard confirmation, a similar peak was explained as a C5 unsaturated carbonyl, generated from addition of the CH_2OO Criegee biradical to 1,3-butadiene at the early stage of the experiment when there was a large amount of 1,3-butadiene and O_3 in the system.

4. Conclusion

Photochemical oxidation of 1,3-butadiene with OH and O_3 has been investigated in this study. In the OH-initiated reaction, carbonyl products, such as glycolaldehyde, glycidaldehyde, glyoxal, butendial, 3-hydroxypropanaldehyde, hydroxy acetone, and malonaldehyde, have been identified and confirmed by their commercial and synthesized standards. Also detected in this experiment were three non-carbonyl compounds, furan, 1,3-butadiene monoxide, and 1,3-butadiene diepoxide.

To understand the photodegradation mechanism of 1,3-butadiene better, two of its immediate products, acrolein and 1,3-butadiene monoxide, have been used to study their own photooxidation processes. In addition, time series of various products have been measured, providing useful information to identify isomers and to understand mechanisms. In two cases where experimental methods are limited, we have used computational chemistry methods to investigate reaction competitions and assist in mechanism interpretations.

References

Acquavella, J.F., 1996. Butadiene epidemiology: a summary of results and outstanding issues. Toxicology 113, 148–156.

Atkinson, R., 1990. Gas-phase tropospheric chemistry of organic compounds: a review. Atmospheric Environment 24A, 1–41.

Atkinson, R., 1997. Gas-phase tropospheric chemistry of volatile organic compounds: 1. Alkanes and alkenes. Journal of physical Chemical Reference Data 26, 215–290.

Atkinson, R., Aschmann, S.M., 1993. OH Radical production from the gas-phase reactions of O_3 with a series of alkenes under atmospheric conditions. Environment Science and Technology 27, 1357–1363.

Atkinson, R., Aschmann, S.M., Arey, J., Tuazon, E.C., 1994a. Formation of epoxides and O (^3P) atoms from the gas-phase reactions of O_3 with a series of alkenes. International Journal of Chemical Kinetics 26, 945–950.

Atkinson, R., Aschmann, S.M., Arey, J., Shorees, B., 1992. Formation of OH radicals in the gas phase reactions of O_3 with a series of terpenes. Journal of Geophysical Research 97, 6065–6073.

Atkinson, R., Aschmann, S.M., Tuazon, E.C., 1994b. Formation of $O(^3P)$ atoms and epoxides from the gas-phase reaction of O_3 with isoprene. Research on Chemical Intermediates 20, 385–394.

Barnes, I., Bastian, V., Becker, K.H., Tong, Z., 1990. Kinetics and products of the reactions of NO_3 with monoalkenes, dialkenes and monoterpenes. Journal of Physical Chemistry 94, 2413–2419.

Bierbach, A., Barnes, I., Becker, K.H., 1995. Product and kinetic study of the OH initiated gas-phase oxidation of furan, 2-methylfuran and furanaldehyde at ≈ 300 K. Atmospheric Environment 29, 2651–2660.

Bond, A.M., Deprez, P.P., Jones, R.D., Wallace, G.G., 1980. Polarographic methods for the determination of propanedial (malonaldehyde). Analytical Chemistry 52, 2211–2213.

Carter, W.P., 1996. Condensed atmospheric photooxidation mechanisms for isoprene. Atmospheric Environment 30, 4275–4290.

Dewar, M.J.S., Zoebisch, E.G., Healy, E.F., Stewart, J.J., 1985. A new general purpose quantum mechanical molecular model Journal of the American Chemical Society 107, 3902–3909.

Fang, J., Vaca, C.E., Valsta, L.M., Mutanen, M., 1996. Determination of DNA adducts of malonaldehyde in humans: effect of dietary fatty acid composition. Carcinogenesis 17, 1035–1040.

Feron, V.J., Til, H.P., de Vrijer, F., Woutersen, R.A., Cassee, F.R., Van Bladeren, P.J., 1991. Aldehydes: occurrence, carcinogenic potential, mechanism of action and risk assessment. Mutation Research 259, 363–385.

Finlayson-Pitts, B.J., Pitts Jr., J.N., 1986. Atmospheric Chemistry: Fundamentals and Experimental Techniques.. Wiley, New York, pp. 636.

Frisch, M.J., Trucks, G.W., Schlegel, H.B., Gill, P.M.W., Johnson, B.G., Robb, M.A., Cheeseman, J.R., Keith, T., Petersson, G.A., Montgomery, J.A., Raghavachari, K., Al-Laham, M.A., Zakrzewski, V.G., Ortiz, J.V., Foresman, J.B., Cioslowski, J., Stefanov, B.B., Nanayakkara, A., Challacombe, M., Peng, C.Y., Ayala, P.Y., Chen, W., Wong, M.W., Andres, J.L., Replogle, E.S., Gomperts, R., Martin, R.L., Fox, D.J., Binkley, J.S., Defrees, D.J., Baker, J., Stewart, J.P., Head-Gordon, M., Gonzalez, C., Pople, J.A., 1995. Gaussian 94, Revision E.1. Gaussian, Inc., Pittsburgh, PA.

Golding, R.T., Kennedy, G., Watson, W.P., 1990. Structure determination of adducts from the reaction of (R)-glycidaldehyde and guanosine. Carcinogensis 11, 865–868.

Golding, B.T., Slaich, P.K., Kennedy, G., Bleasdale, C., Waston, W.P., 1996. Mechanisms of formation of adducts from reactions of glycidaldehyde with 2′ deoxyguanosine and/or guanosine. Chemical Research in Toxicology 9, 147–157.

Grosjean, D., 1990. Atmospheric chemistry of toxic contaminants. 3. Unsaturated aliphatics: acrolein, acrylonitrile, maleic anhydride. Journal of Air and Waste Management Association 40, 1522–1531.

Grosjean, D., Grosjean, E., Williams, II. E.L., 1994a. Atmospheric chemistry of olefins: a product study of the ozone-alkene reaction with cyclohexane added to scavenge OH. Environmental Science and Technology 20, 186–196.

Grosjean, E., Williams, II.E.L., Grosjean, D., 1994b. Atmospheric chemistry of acrolein. Science of the Total Environment 153, 195–202.

Gutteridge, J.M.C., 1975. The use of standards for malonyldialdehyde. Analytical Biochemistry 69, 518–526.

Jeffries, H.E., 1995. Phtotchemical air pollution. In: Singh, H.B. (Ed.) Composition, Chemistry, and Climate of the Atmosphere. Van Nostand-Reinhold, New York (Chapter 9).

Jeffries, H.E., Fox, D.L., Kamens, R.M., 1976. Outdoor smog chamber studies: light effects relative to indoor chambers. Environmental Science and Technology 10, 1006–1011.

Kligerman, A.D., Doerr, C.L., Milholland, V.S., Tennant, A.H., 1996. Cytogenetic effects of butadiene metabolites in rat and mouse splenocytes following in vitro exposures. Toxicology 113, 336–340.

Knaap, A.G.A.C., Voodg, C.E., Kramers, P.G.N., 1982. Comparision of the mutagenic potency of 2-chloroethanol, 2-bromoethanol, 1,2-epoxybutane, epichlorohydrin and glycidaldehyde in Klebsiella Pneumoniae, Drosophila Melanogaster and L5178Y mouse Lymphoma cells. Mutation Research 101, 199–208.

Maldotti, A., Chiorboli, C., Bignozzi, C.A., Bartocci, C., Carassiti, V., 1980. Photooxidation of 1,3-butadiene containing systems: rate constant determination for the reaction of acrolein with OH radicals. International Journal of Chemical Kinetics 12, 905–913.

Martinez, R.I., Herron, J.T., Huie, R.E., 1981. The mechanism of ozone-alkene reactions in the gas phase. A mass spectrometric study of the reactions of eight linear and branched-chain alkenes. Journal of the American Chemical Society 103, 3807–3820.

McCann, J., Choi, E., Yamasaki, E., Ames, B.N., 1975. Detection of carcinogens as mutagens in the salmonella/microsome test: assay of 300 chemicals. Proceedings of the National Academy of Science USA 72, 5135–5139.

Nishiyama, T., Hagiwara, Y., Hagiwara, H., Shibamoto, T., 1994. Formation and inhibition of genotoxic glyoxal and malonaldehyde from phospholipids and fish liver oil upon lipid peroxidation. Journal Agricultural and Food Chemistry 42, 1728–1731.

Ohta, T., 1983. Rate constants for the reactions of diolefins with OH radicals in the gas phase. Estimate of the rate constants from those for monoolefins. Journal of Physical Chemistry 87, 1209–1213.

Ohta, T., 1984. Furan ring formation in OH-initiated photooxidation of 1,3-butadiene and cis-1, 3-pentadiene. Bulletin of the Chemical Society of Japan 57, 960–966.

Osterman-Golkar, S., Bond, J.A., 1996. Biomonitoring of 1,3-butadiene and related compounds. Environmental Health Perspectives 104 (Suppl. 5), 907–915.

Paulson, S.E., Flagan, R.C., Seinfeld, J.H., 1992a. Amospheric photooxidation of isoprene Part I: The hydroxyl radical and ground state atomic oxygen reactions. International Journal of Chemical Kinetics 24, 79–101.

Paulson, S.E., Flagan, R.C., Seinfeld, J.H., 1992b. Amospheric photooxidation of isoprene Part II: The ozone-isoprene reaction. International Journal of Chemical Kinetics 24, 103–125.

Recio, L., Meyer, K.G., Pluta, L.J., Moss, O.R., Saranko, C.J., 1996. Assessment of 1,3-butadiene mutagenicity in the bone marrow of B6C3F1/ac/transgenic mice (big blue): a review of mutational spectrum and /ac/ mutant frequency after a 5-day 625ppm 1,3-butadiene exposure. Environmental and Molecular Mutagenesis 28, 424–429.

Skov, H., Hjorth, J., Lohse, C., Jensen, N.R., Restelli, G., 1992. Products and mechanisms of the reactions of the nitrate radical (NO_3) with isoprene, 1,3-butadiene and 2,3-dimethyl-1, 3-butadiene in air. Atmospheric Environment 26A, 2771–2783.

Sorsa, M., Peltonen, K., Anderson, D., Demopoulos, N.A., Neumann, H.-G., Osterman-Golkar, S., 1996. Assessment of environmental and occupational exposures to butadiene as a model for risk estimation of petrochemical emissions. Mutagenesis 11, 9–17.

Thornton-Manning, J.R., Dahl, A.R., Bechtold, W.E., Griffith, W.C., Henderson, R.F., 1997. Comparison of the disposition of butadiene epoxides in sprague-dawley rats and B6C3F$_1$ mice following a single and repeated exposures to 1,3-butadiene via inhalation. Toxicology 123, 125–134.

Wayne, R.P., Barnes, I., Biggs, P., Burrows, J.P., Canosa-Mas, C.E., Hjorth, J., Le Bras, G., Moortgat, G.K., Perner, D., Poulet, G., Restelli, G., Sidebottom, H., 1991. The nitrate radical: physics, chemistry, and the atmosphere. Atmospheric Environment 25A, 1–203.

Wiesen, E., Barnes, I., Becker, K.H., 1995. Study of the OH initiated degradation of the aromatic photooxidation product 3,4-dihydroxy-3-hexene-2, 5-dione. Environmental Science and Technology 29, 1380–1386.

Yu, J., Jeffries, H.E., 1997. Atmospheric photooxidation of alkylbenzenes-II. Evidence of formation of epoxide intermediates. Atmospheric Environment 31, 2281–2287.

Yu, J., Jeffries, H.E., Le Lacheur, R.M., 1995. Identifying airborne carbonyl compounds in isoprene atmospheric photooxidation products by their PFBHA oximes using gas chromatography/ion trap mass spectrometry. Environmental Science and Technology 29, 1923–1932.

Yu, J., Jeffries, H.E., Sexton, K.G., 1997. Atmospheric photooxidation of alkylbenzenes-I. Carbonyl products analyses. Atmospheric Environment 31, 2261–2280.